Eksakta : Berkala Ilmiah Bidang MIPA
VOLUME 27 NO 04 2026, pp 771-789
ISSN : Print 1411-3724 — Online 2549-7464
DOI : https://doi.org/10.24036/eksakta/vol27-iss04/742

Eksakta
Berkala Ilmiah Bidang MIPA
http://www.eksakta.ppj.unp.ac.id/index.php/eksakta

Article

Integrating Time-Dependent and Time-Independent Earthquake Recurrence Models for Fault-Based Seismic Hazard Mapping in Indonesia

Rafif Rahmat Ramadhan[1], Rizki Wulandari[1,2*], Yudha Styawan[1,2], Purwaditya Nugraha[1], Meta Nisrina Syafitri[1]

[1]Department of Geophysical Engineering, Faculty of Industrial Technology, Institut Teknologi Sumatera, Lampung, Indonesia
[2]Center for Earthquake and Tsunami Disaster Mitigation, Institut Teknologi Sumatera, Lampung, Indonesia

Article Info

Article history :
Received August 10, 2026
Revised August 20, 2026
Accepted August 24, 2026
Published August 30, 2026

Keywords :
Brownian passage time,
poisson model,
faults, earthquake,
peak ground acceleration

Abstract. Indonesia requires precise seismic hazard assessments to mitigate risks from extreme tectonic plate convergence. Currently, standard mapping heavily relies on time-independent Poisson models, which ignore the elapsed time since historical earthquakes and fail to capture cyclic fault behavior. Updating national hazard maps urgently demands time-dependent approaches. Therefore, this research integrates Poisson and Brownian Passage Time (BPT) models across active faults in Indonesia to dynamically evaluate rupture probabilities and enhance probabilistic seismic hazard assessment (PSHA). Earthquake catalogs (1900–2025) and national fault parameters were processed using OpenQuake. Crucially, the BPT approach estimates rupture probability from tectonic stress accumulation, recurrence intervals, elapsed time, and an aperiodicity parameter (α=0.5) characterizing cycle variability. Results demonstrate the BPT model's sensitivity in identifying late-cycle faults, projecting >90% rupture probabilities for the Aceh-South and Batee A segments, while confirming significant hazard reductions (3.75%) for early-cycle faults like Palu-Saluki. To maintain comprehensive coverage, the Poisson model generated a broader baseline hazard distribution, yielding peak ground accelerations (PGA) exceeding 1.35 g at a 2% probability of exceedance in 50 years on Northern Sumatera faults. Integrating these complementary models produces cycle-consistent spatial hazard patterns, providing a robust foundation for national infrastructure planning.

Corresponding Author :
Rizki Wulandari
Department of Geophysical Engineering, Faculty of Industrial Technology,
Institut Teknologi Sumatera, Lampung, Indonesia
Email : rizki.wulandari@tg.itera.ac.id

1. Introduction

Indonesia sits at the intersection of three major tectonic plates: the Indo-Australian, Eurasian, and Pacific plates. This setting produces a dense network of active faults and subduction zones across the archipelago. The Sumatran Faults System alone extends over 1,900 km, and active faults are also mapped in Java, Sulawesi, and Nusa Tenggara [1-2]. Earthquake magnitudes generated by this system range from small intraplate events to subduction-zone earthquakes of Mw 9 or larger. Given the high seismic potential and dense population near these faults, understanding recurrence patterns is essential for disaster mitigation and infrastructure planning.

Standard Probabilistic Seismic Hazard Assessment (PSHA) typically models earthquake occurrence as a time-independent Poisson process [3-4]. This assumption treats rupture as memoryless, unaffected by the time elapsed since the last event. It does not reflect Elastic Rebound Theory, under which fault stress dissipates after rupture and reaccumulates over time [5]. Rupture probability should therefore rise as elapsed time increases. Time-dependent renewal models were developed to capture this behavior, most notably the Brownian Passage Time (BPT) model, which represents the earthquake cycle as a Brownian relaxation-oscillator process governed by a mean recurrence interval and an aperiodicity parameter [6].

Several renewal models besides BPT have been proposed, including the Lognormal, Gamma, and Weibull distributions [4], [7]. BPT is adopted here for three reasons. First, its hazard function approaches a finite, non-zero value at long elapsed times, unlike the Lognormal model, whose hazard falls toward zero and contradicts elastic-rebound reasoning [4], [7]. Second, evaluations for complex fault systems such as the Uniform California Earthquake Rupture Forecast found that BPT, Weibull, Gamma, and Normal models perform comparably near the mean recurrence interval, so model choice is not a major source of epistemic uncertainty [8]. BPT additionally allows stress-transfer effects from prior earthquakes to be incorporated directly, a feature not readily available under the Lognormal formulation. Third, BPT has become the standard renewal model in recent time-dependent PSHA studies, including hybrid frameworks combining BPT with aftershock models [9], which supports comparability with the wider literature.

Global studies have repeatedly shown the value of time-dependent models over Poissonian ones alone. In California, the Working Group on California Earthquake Probabilities and the UCERF3 model improved estimates of fault readiness and multi-fault rupture potential [10-11]. Time-dependent behavior has further been validated through direct geodetic strain measurements along the Parkfield segment [12]. In the Cascadia Subduction Zone, time-dependent probabilities modulated by episodic slow-slip events have improved hazard estimates [13]. Comparable gains have been reported for layered fault-based analyses in Central Italy [14] and for hazard simulations in the Marmara Sea, Turkey, incorporating post-Izmit stress-transfer effects [15].

Within Indonesia, a recent fault-based assessment integrated Poissonian and BPT models across 28 fault segments in Lampung and southern Sumatra [16]. Elapsed-time information produced more cycle-consistent spatial hazard patterns than Poissonian estimates alone, consistent with earlier BPT rupture-probability work following the 2022 Mw 6.2 Pasaman earthquake sequence [17]. Both studies report improved hazard representation in late-cycle segments, where 50-year rupture probabilities exceed 50%, and reduced overestimation in early-cycle segments. Peak ground acceleration (PGA) for a 2% probability of exceedance in 50 years reaches 0.6–1.5 g adjacent to the Sumatran Fault System [16]. These results confirm the value of time-dependent modeling, but only at a single regional scale.

Scaling this approach to the hundreds of fault segments mapped across Indonesia is not a direct extrapolation. The Lampung assessment relies on a relatively well-constrained record of each segment's most recent rupture, but comparable data are far scarcer nationally. Systematic historical earthquake catalogs for Indonesia extend reliably back only to the mid-seventeenth century [1]. Paleoseismic trenching, the primary method for dating pre-instrumental ruptures, has been completed on only a small fraction of mapped segments, with new results still being added [18]. This mirrors a broader challenge in time-dependent hazard modeling: renewal-model parameters are difficult to constrain wherever paleoseismic records are sparse or unevenly distributed [19]. No prior hazard assessment study, including the Lampung-scale work above, has articulated how segments with dated ruptures should be treated differently from segments where elapsed time remains unknown.

This gap is timely to address given Indonesia's newly completed national hazard update in 2024, consolidating new active-fault, and strong-motion data nationwide [20]. This update makes a nationwide time-dependent analysis feasible for the first time. However, it continues to apply a time-independent framework to most fault sources, leaving the integration of elapsed-time information as an open problem rather than a resolved one. Addressing this problem is the specific novelty pursued in this study.

This study aims to integrate time-dependent (BPT) and time-independent (Poissonian) recurrence models across Indonesia's active fault system, using the 2024 national fault source database. It evaluates how elapsed time since the most recent known rupture, where available, influences the probability of future seismic events. It also proposes a transparent treatment for fault segments where elapsed-time data remain limited or absent. By coupling time-dependent modeling with the standard PSHA framework at national scale, this study aims to improve current understanding of potential ground-motion levels across Indonesia's active faults and to provide a methodological basis for future assessments facing incomplete elapsed-time data.

2. Experimental Section

2.1. Research Area

Earthquake data were obtained from the International Seismological Centre (ISC), the United States Geological Survey (USGS), Gempa Nusantara [1], and Indonesian Agency for Meteorology, Climatology, and Geophysics (BMKG). The data covers the territory of Indonesia (6° N – 11° S, 95° – 141° E) for the period from 1900 to 2025, with magnitudes ranging from 0 to 10 and depths ranging from 0 to 50 km.

2.2. Theoretical Research

Earthquake data are limited to depths of 0–50 km, a range that represents the boundaries of the Earth's brittle crust where the majority of shallow fault earthquakes occur, as deformation below this zone transitions into ductile strain localization processes rather than brittle rupture [21-23]. In addition, catalog data, used as a source of historical earthquake information, were also integrated from various sources. The earthquake data obtained from these various sources must then be harmonized into a single scale (M_W) as a conversion reference using the empirical magnitude relationships, as presented in Table 1, adopted in the 2024 national earthquake source and hazard map guidelines [20]. This magnitude harmonization aims to maintain consistency among the catalog data.

Table 1. Empirical formulas for converting various earthquake magnitude scales (M_b, M_s, M, M_L) to Moment Magnitude (M_W) along with their applicable magnitude ranges [20].

Magnitude Conversion	Empirical Formula	Magnitude Scale
M_b to M_W	M_W=0.7212M_b+1.4433	2≤M_b ≤3.6
M_b to M_W	M_W=1.0107M_b+0.0801	3.7≤M_b ≤10
M_s to M_W	M_W=0.6016M_s+2.476	2≤M_s ≤6
M_s to M_W	M_W=0.9239M_s+0.5671	6.1≤M_s≤10
M to M_W	M_W=1.0166M+0.2207	2.7≤ M ≤10
M_L to M_W	M_W=0.7473M_L+1.0651	3≤M_L≤7.9

Declustering refines the catalog to isolate independent mainshocks. The Reasenberg method effectively defines spatio-temporal linkages between seismic events [21-22]. It applies dynamic spatial interaction zones and magnitude-dependent temporal windows [24]. Prior to declustering, the magnitude of completeness (M_c) was evaluated. The M_c ranges from 4.5 to 5.0 for the instrumental era. Figure 1 illustrates the final spatial distribution.

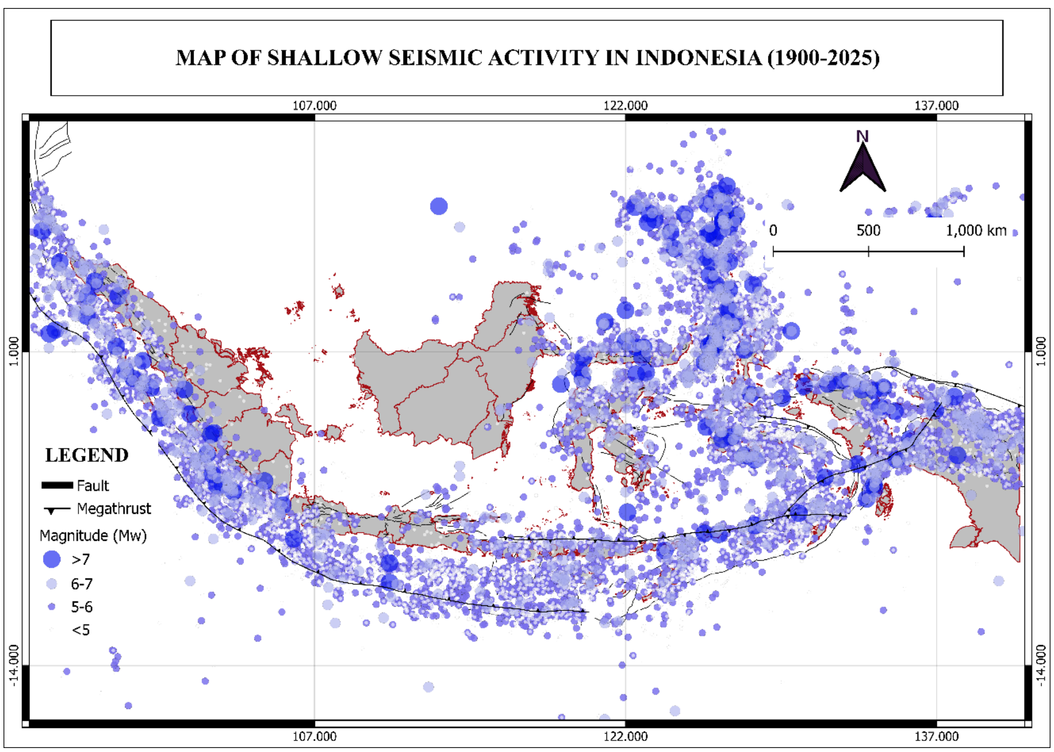

Figure 1. Distribution of earthquake epicenters (Mw 5 – 8.6) in Indonesia. Fault lines are shown in thick black, subduction zones are marked with thin black lines, and provincial boundaries are marked with gray lines. The earthquakes shown represent shallow earthquakes with depths of up to 50 km.

Main fault data originate from the 2024 Assessment earthquake source map [20],[25]. Collected parameters include segment length, orientation, slip mechanism, and annual slip rate. The dataset encompasses major regional active fault systems. These include the Andaman, Philippine, and Papua fault networks. In total, 401 active fault records were rigorously analyzed.

Table 2. 31 Segments of Active Fault

ID	Name	Segment	Type	Dip (°)	Width (km)	Length (km)	Maximum Magnitude	Slip rate mm/year	Historical Events			
									Date	Source	Mag	Elapsed time until 2025
1	Sumatran Fault	Seulimeum-South	SS	90	20	38	6.8	6	22/10/2013	ISC	5.5	12
2	Pidie Fault	Pidie Jaya	SS	90	20	23	6.5	1	12/04/1967	USGS	6.7	58
3	Pidie Fault	Panteraja	SS	90	23	23	6.5	1	06/12/2016	USGS	6.5	9
4	Sumatran Fault	Tripa-Thrust	R	45W	30	33	6.8	16	13/09/2020	ISC	5.1	5
5	Sumatran Fault	Aceh-South	SS	90	20	27	6.6	14	02/01/2012	ISC	5.4	13
6	Sumatran Fault	Batee A	SS	90	20	45	6.7	6	03/08/1935	USGS	7	90
7	Sumatran Fault	Batee B	SS	90	20	50	6.2	0.5	17/04/1934	USGS	5.8	91
8	Lhokseumawe Fault	Lhokseumawe A	SS	90	20	37	6.8	1	23/08/1936	Gempa Nusantara	-	89
9	Lhokseumawe Fault	Lhokseumawe B	SS	90	20	25	6.5	0.5	23/08/1936	Gempa Nusantara	-	89
10	Lhokseumawe Fault	Lhokseumawe C	SS	90	20	19	6.4	0.5	23/08/1936	Gempa Nusantara	-	89
11	Takengon Fault	Lot Tawar-B	SS	90	20	22	6.5	1	19/09/2008	USGS	5.2	17
12	Sumatran Fault	Tripa 5	SS	90	20	21	6.5	8	15/11/1990	ISC	6.6	35
13	Oreng Fault	Oreng SS	SS	90	20	62	6.8	1	20/11/1994	ISC	6.1	31
14	Sumatran Fault	Toru-2	SS	90	20	29	6.6	9.3	11/08/2021	ISC	4.9	4
15	Sumatran Fault	Sumpur	SS	90	20	48	6.7	14	25/02/2022	ISC	6.1	3
16	Sumatran Fault	Angkola-South B	SS	90	20	30	6.6	5	06/06/1984	USGS	5.1	41
17	Sumatran Fault	Semangko Timur-A	SS	90	20	94	6.1	3	02/04/1919	USGS	6.5	106
18	Tampomas	Tampomas	N	60	30	8	5.6	0.5	---	-	-	-
19	Rawapening Fault	Rawapening	SS	45	30	20	5.9	1.5	---	-	-	-
20	Mataram Fault	Tambakbayan	SS-LL	90	30	14	6.1	1	---	-	-	-
21	Bawean	East Bawean	R	45SE	20	103	7.5	0.1	06/06/2004	ISC	5.9	21
22	Karangmanggu Fault	Karangmanggu	SS	90	20	20	6.1	0.5	---	-	-	-
23	Lembang Fault	Lembang	SS	90	20	30	6.6	3.45	16/09/1998	USGS	4.5	27
24	Cianjur Fault	Cianjur 2	SS	90	20	5	5.6	0.1	21/11/2022	ISC	5.6	3
25	Wonsorejo Fault	Wonsorejo	SS	90	25	11	5.9	0.225	---	-	-	-
26	Palukoro	Palu-Saluki	SS	90	20	176	7.7	40	28/09/2018	ISC	7.6	7
27	Matano	Kolono-1	SS	90	20	32	6.7	20	---	-	-	-
28	Sorong Fault	West Salawati	SS	90	20	45	6.8	30	---	-	-	-
29	Sorong Fault	Meuni	SS	90	20	23	6.5	10	14/04/1932	USGS	5.8	93
30	Wapoga	Wapoga	SS	90	20	252	7.9	60	26/11/2004	ISC	7.1	21
31	Mamberamo	Mamberamo	SS	90	20	133	7.5	70	27/06/1987	ISC	6.5	38

Note: Several parameters of active faults in Indonesia were used in earthquake source modeling for this study, including segment name, fault type, dip angle, maximum magnitude, slip rate, and historical earthquake data. Time elapsed since the last event. Fault parameter and historical earthquake data were collected from the USGS, ISC, and PuSGeN 2024. The table contains 31 of 401 faults, based on the most significant results. Fault types are abbreviated as follows: SS (Strike-Slip), R (Reverse), SS-LL (Strike-Slip Left-Lateral), and N (Normal).

Recurrence intervals were calculated based on established fault parameters. This defines the expected time between consecutive earthquakes on a segment. The estimation follows a statistical framework using historical seismic data [26]. Earthquake recurrence intervals are normalized relative to their average. The mathematical relationship is expressed in Equation (1).

$$RI = \frac{10^{b \cdot Mmax} - 10^{c + d \cdot M}}{slip\ rate} \quad (1)$$

In Equation (1), RI represents the recurrence interval. The variable M is the characteristic earthquake magnitude. Parameters M_{max} denotes the maximum credible earthquake magnitude the fault can theoretically generate. Variables b are b-value=0.89, c, and d are empirical scaling constants (Table 3). The parameter *Slip rate* represents the annual fault slip rate.

Table 3. Empirical scaling constants (c and d) utilized in the scaling law for slip-magnitude relations, categorized by the type of fault slip mechanism.

Fault Type	c	d
Strike-slip	-6.32	0.9
Reverse	-0.74	0.08
Normal	-4.45	0.63
All	-4.8	0.69

The Poisson model provides a baseline probabilistic approach for hazard Assessment [4]. It assumes earthquake events occur randomly and independently. This model incorporates no statistical memory of previous seismic events. The regional earthquake occurrence rate remains constant over time. Its probability over a time interval t is calculated using Equation (2).

$$P(t) = 1 - e^{-\lambda t} \tag{2}$$

In Equation (2), t is the prediction time interval or duration. The variable λ represents the annual occurrence rate of earthquakes, e is Euler's number ($e \approx 2.718$). The Brownian Passage Time (BPT) model represents time-dependent earthquake cycles. It models structural stress accumulation as a Brownian random process. Earthquakes trigger when accumulated stress reaches a specific threshold. The aperiodicity parameter (α) was set to 0.5, aligning with standard USGS evaluation guidelines [25]. The probability density function is presented in Equation (3).

$$f(t) = \frac{1}{\sqrt{2\pi\alpha t}} \exp\left(-\frac{(t-\mu)^2}{2(\alpha\mu)^2 t}\right) \tag{3}$$

In Equation (3), the variable t is the elapsed time since the last major earthquake. The parameter μ denotes the average recurrence interval. The coefficient α defines the aperiodicity variance of the seismic cycle.

Hazard curves evaluate the annual exceedance rate of ground motion intensity. This numerical calculation integrates sources, occurrence rates, and conditional probabilities. Equation (4) defines this comprehensive regional integration process [27]. Shallow crustal faults employed a logic tree equally weighting the Chiou-Youngs 2014, Campbell-Bozorgnia 2014, and Boore-Atkinson 2014 Ground Motion Prediction Equations.

$$\lambda(IM > x) = \sum_{i=1}^{Ns} vi \int_{Mmin}^{Mmax} \int_{0}^{rmax} P(IM > x|m,r) \cdot f_M(m) \cdot f_R(r)\, dr\, dm \tag{4}$$

In Equation (4), $\lambda(IM > x)$ represents the annual exceedance rate. The variable N_s is the total number of seismic sources. and v_i denotes the annual earthquake occurrence rate at the i-th source. The conditional probability of exceedance is denoted by $P(IM > x|m,r)$. Magnitude and distance probability density functions are represented by $f_M(m)$ and $f_R(r)$ [27].

The PSHA calculations were performed using the OpenQuake engine developed by the Global Earthquake Model (GEM) Foundation [28], an open-source platform for earthquake hazard and risk assessment. This generates hazard maps that display the geographic distribution of earthquake hazard levels based on PGA values at each location. Through these maps, differences in hazard levels between regions can be clearly identified, facilitating the identification of areas with high and low hazard levels.

The integration of the Brownian Passage Time and Poissonian models is performed to optimize seismic hazard assessments while addressing the limitations of historical earthquake data completeness in Indonesia. Within the Probabilistic Seismic Hazard assessment framework using the OpenQuake Engine, the Brownian Passage Time model is prioritized as the primary approach because it calculates probability values using a physically more accurate method. This model evaluates earthquake occurrence probabilities dynamically according to the maturity of the fault strain cycle. If a fault segment lacks sufficient historical earthquake records to determine the exact elapsed time since the last major rupture, the Poisson model will replace the Brownian Passage Time model for that specific segment in OpenQuake.

Calculated PGA data undergoes extensive spatial interpolation. This generates continuous hazard maps across the designated study area. Results highlight probabilities of 10.0% and 2.0% exceedance in 50 years. Public infrastructure design strictly follows the 10.0% probability threshold [29]. Conversely, high-damage structural modeling relies on the stricter 2.0% parameter.

Ideally, time-dependent renewal models require maximum magnitude (M_{max}) characteristic earthquakes to signify a complete reset of the tectonic stress cycle. However, due to the temporal limitations of instrumental earthquake catalogs in Indonesia—which rarely span full millennial seismic cycles, relying exclusively on M_{max} events is impractical. Therefore, this study incorporates moderate-to-small historical earthquakes, including documented events below Mw 5.0, as temporal anchors for the elapsed time parameter. These lower-magnitude events still represent critical localized stress drops and partial strain release along the fault's asperities. Furthermore, on comparatively short fault segments with lower slip rates, events below Mw 5.0 can account for a substantial proportion of the segment's total seismic capacity. Consequently, in the absence of complete paleoseismic records, utilizing these events provides the most robust and data-driven probabilistic proxy to initialize the Brownian Passage Time hazard calculations.

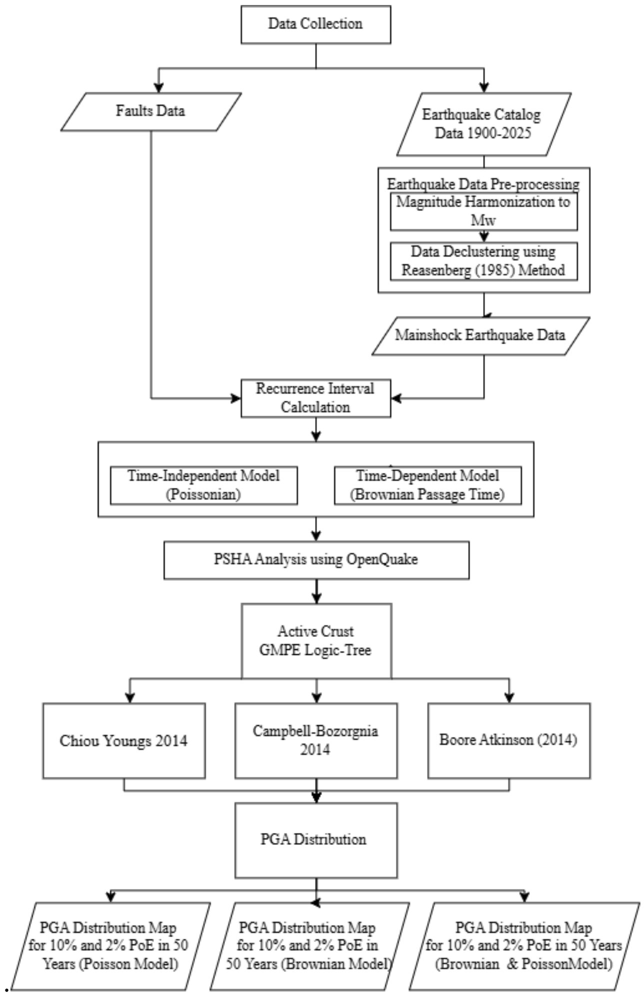

Figure 2. Research Workflow

3. Results and Discussion

On Figure 3 and Table 4, the time-dependent BPT model on northern Sumatera projects near-certain 50-year rupture probabilities for the Batee A (ID 6) and Aceh-South (ID 5) segments, yielding 99.57% and 99.99% PoE respectively. These values significantly exceed their baseline Poissonian probabilities. Both segments are currently in a highly overdue, late-cycle state. The Batee A segment has accumulated strain for 90 years—more than four times its 20-year recurrence interval. Similarly, the Aceh-South segment, driven by a high slip rate of 14 mm/year, has surpassed its 4-9 year recurrence interval with 13 years elapsed since its last rupture in 2012.

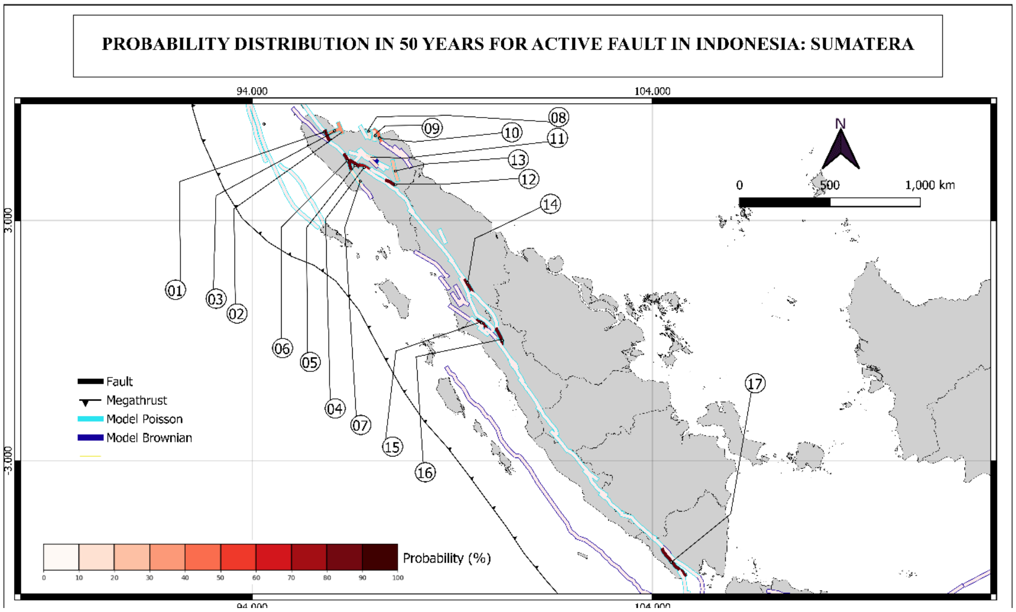

Figure 3. Map showing the spatial distribution of the 50-year fault probability for all major active faults in Sumatera based on a combined Poisson and BPT recurrence model. Segments 1-17.

These high time-dependent probabilities align directly with recent paleoseismic trenching and fault mapping along the Aceh Fault system [18], which identified critical overdue faulting dynamics within the Great Sumatran Fault network. The physical maturity of these segments corroborates established historical seismicity patterns [2]. Because these segments form a continuous 300 km seismic hazard belt, spatial planning and infrastructure design in Aceh must abandon baseline averages and strictly implement maximum Peak Ground Acceleration (PGA) parameters to withstand imminent moderate-to-large (Mw 6.1–6.8) events.

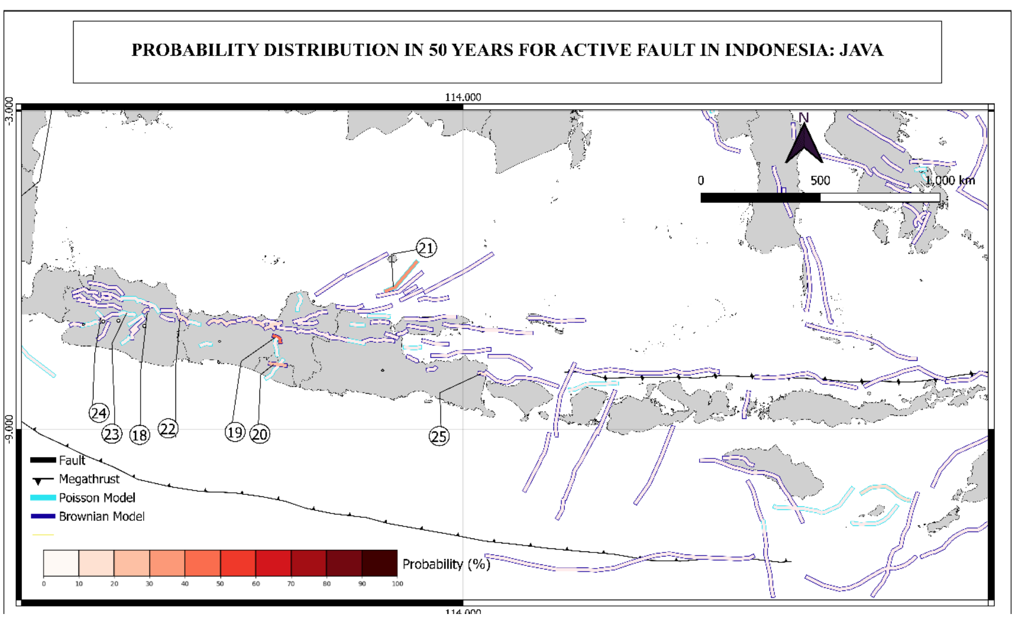

Figure 4. Map showing the spatial distribution of the 50-year fault probability for all major active faults in Java based on a combined Poisson and BPT recurrence model. Segments 18-25.

The Western Java region demonstrates asymmetric hazard profiles, with the Cianjur 2 segment (ID 24) showing a near-zero BPT PoE (3.9×10^{-7}%) compared to a Poisson PoE of 9.09%. This segment is firmly in an early-cycle phase. The devastating 2022 Mw 5.6 Cianjur earthquake successfully depleted localized tectonic stress, resulting in an elapsed time of only 3 years against a long average recurrence interval.

This early-cycle drop in calculated hazard reflects the foundational elastic rebound principles, where accumulated strain is reset following major crustal ruptures. Despite the low immediate time-dependent rupture probability, the 2022 event proved that even shallow, moderate energy releases along low slip-rate faults (0.1 mm/year) can cause catastrophic damage. Therefore, mitigation strategies in densely populated areas like Greater Bandung, intersected by faults like Lembang (ID 23) must utilize the more conservative Poisson baseline to protect fragile infrastructure from cascading crustal interactions.

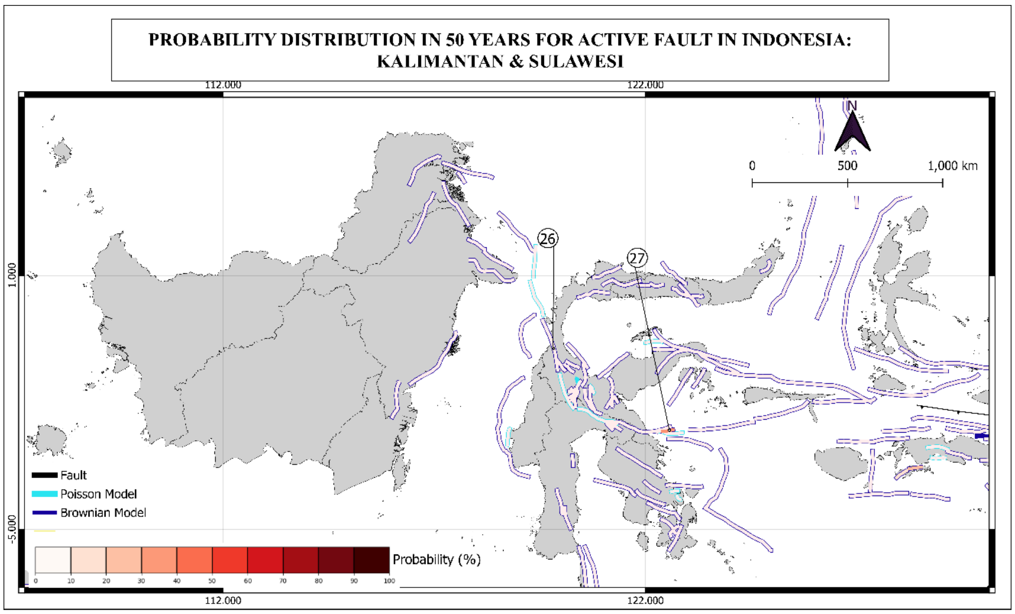

Figure 5. Map showing the spatial distribution of the 50-year fault probability for all major active faults in Sulawesi and Kalimantan based on a combined Poisson and BPT recurrence model. Segments 26-27.

The Palu-Saluki segment (ID 26) of the Palukoro Fault demonstrates a drastic reduction in seismic hazard under time-dependent modeling, dropping from a Poisson PoE of 28.9% to a BPT PoE of just 3.75%. The segment is characterized by an early-cycle dynamic. The massive release of energy during the 2018 Mw 7.6 Palu earthquake effectively reset the fault's stress accumulation, leaving an elapsed time of only 7 years relative to a highly active slip rate of 40 mm/year.

This quantifiable reduction in time-dependent hazard is consistent with global comparisons of paleoearthquake elapsed times and mean interevent-times [19], which indicate that large-magnitude ruptures reliably depress immediate subsequent rupture probabilities. While the short-term rupture probability is drastically reduced, the segment's extensive length (176 km) and high potential magnitude (Mw 7.7) necessitate that ongoing post-disaster reconstruction in Palu, Donggala, and surrounding cities relies on the time-independent baseline, ensuring long-term structural resilience against future cycles.

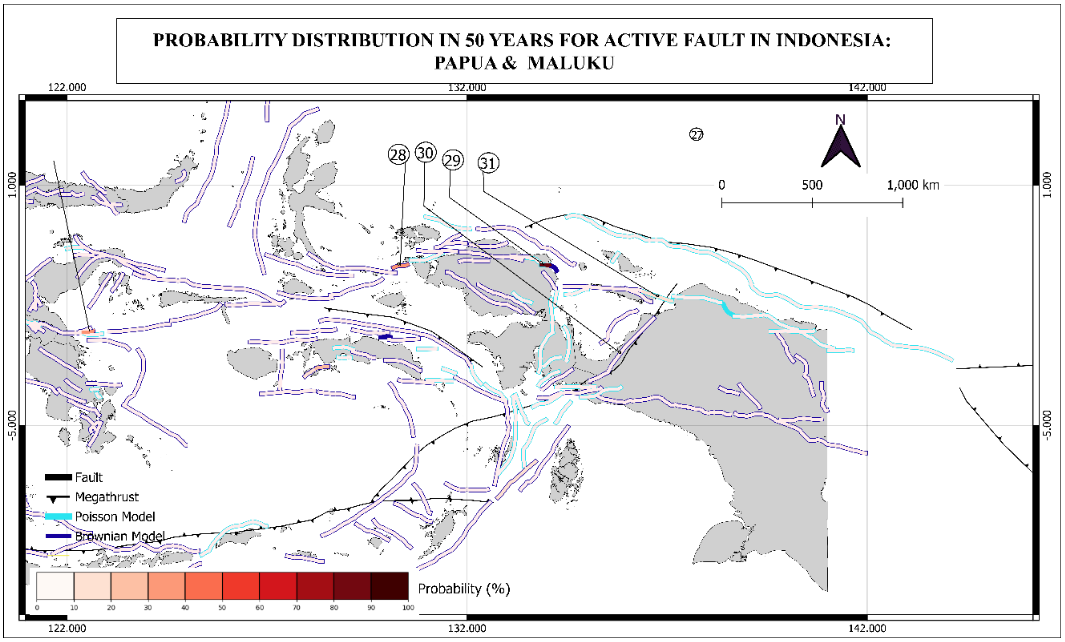

Figure 6. Map showing the spatial distribution of the 50-year fault probability for all major active faults in Papua and Maluku based on a combined Poisson and BPT recurrence model. Segments 28-31.

Within the highly complex Sorong cluster, the Sorong Fault-Meuni segment (ID 29) exhibits a severe BPT PoE of 96.41%, notably higher than its Poisson PoE of 77.13%. This segment represents the most mature fault identified in eastern Indonesia; it is in an extreme late-cycle phase. With 93 years elapsed since its last known rupture in 1932, it has heavily exceeded its calculated mean recurrence interval of 15 years, driven by a rapid slip rate of 10 mm/year.

The extreme discrepancy between the BPT and Poisson models for the Sorong-Meuni segment underscores the necessity of incorporating historical elapsed time data into PSHA, a limitation noted in recent national seismic source updates (PuSGeN 2024). The maturity of this segment mirrors the overdue physical states identified in global paleoseismicity datasets [19]. The "Bird's Head" region of Papua faces imminent critical strain release. Hazard mitigation protocols in this specific cluster cannot rely on baseline Poissonian mapping; instead, engineering parameters must urgently be upgraded to accommodate the maximum expected PGA corresponding to a late-cycle M 6.5 event.

Table 4. Estimated probabilistic seismic hazard parameters for active fault segments (IDs 1-7). The values compare the annual rate, probability of exceedance (PoE) in 50 years, and recurrence interval generated by the Poissonian model against the Brownian Passage Time (BPT) model. Missing data for certain segments is due to the absence of historical earthquake records.

I	Poisson Model			Brownian Passage Time Model		
	Annual Rate	PoE in 50 years (%)	Recurrence Interval (years)	Annual Rate	PoE in 50 years (%)	Recurrence Interval (years)
1	0.0499	91.75	20	0.1069	99.5	9
2	0.00832	34.02	120	0.0121	45.4	83
3	0.00832	34.02	120	0.0022	10.39	455
4	0.02912	76.67	34	0.04373	88.76	23
5	0.11645	99.7	9	0.25876	99.99	4
6	0.04991	91.75	20	0.10937	99.57	9
7	0.00416	18.77	240	0.00358	16.36	280
8	0.00832	34.02	120	0.01574	54.48	64
9	0.00416	18.77	240	0.00345	15.83	290
10	0.00416	18.77	240	0.00345	15.83	290
11	0.00832	34.02	120	0.00355	16.27	281
12	0.06654	96.41	15	0.14884	99.94	7
13	0.00832	34.02	120	0.00654	27.89	153
14	0.07735	97.9	13	0.15991	99.96	6
15	0.11645	99.7	9	0.24763	99.9	4
16	0.04159	87.49	24	0.09418	99.09	11
17	0.02495	71.28	40	0.05635	94.02	18
18	0.00418	18.85	239	-	-	-
19	0.01535	53.58	65	-	-	-
20	0.00676	28.68	148	-	-	-
21	4.17×10^{-6}	0.02	239565	-	-	-
22	0.00338	15.55	296	-	-	-
23	0.00414	18.71	241	0.00025	1.24	4002
24	0.0019	9.09	525	3.0×10^{-10}	3.9×10^{-7}	3.5×10^{9}
25	0.0023	10.87	434	-	-	-
26	0.0068	28.9	147	0.00076	3.75	1308
27	0.01302	47.87	76	-	-	-
28	0.01193	44.92	84	-	-	-
29	0.02951	77.13	34	0.06	96.41	15
30	0.00066	3.242	1517	-	-	-
31	0.00239	11.27	418	0.00001	0.04843	103211

Figure 7 shows an earthquake hazard map of Indonesia with a 10% probability of exceedance in 50 years. This map is based on annual event data obtained from a Poissonian probability model. The data shown on the map indicate PGA contours that are more extensive and widespread. In northern

Sumatera, the areas adjacent to the Seulimeum-South, Tripa-Thrust, Aceh-South, Batee, and Lhokseumawe A segments (IDs 1, 4, 5, 6, 8), form a continuous fault extending approximately 300 km across the Aceh mainland, with acceleration values ranging from 0.6 to over 1.35 g. The highest annual rates in Java region are found along the Tampomas Fault (0.00418) (ID 18), rawapening (ID 19) (0.01535), and Lembang Fault (ID 23) (0.004143). In Central Sulawesi (Palukoro (ID 26)), the region also stands out with PGA values in the Poisson model exceeding 1 g. This is due to the high slip rate (40 mm/year). With Mmax values of 7.3–7.7, the radius of influence is extensive, encompassing the cities of Palu, Donggala, Parigi, Poso, and Luwuk—all of which fall within the 0.15–0.45 PGA zone.

The Poisson baseline (Figures 7 and 8) establishes a widespread, uninterrupted hazard envelope, generating peak ground accelerations (PGA) exceeding 1.35 g at a 2% probability of exceedance (PoE) along the Sumatran fault and over 1.0 g along the Palukoro fault. This time-independent approach inherently assumes a constant rate of tectonic strain release. It effectively treats all fault segments as if they are in identical phases of stress accumulation, ignoring whether a segment ruptured yesterday or centuries ago.

When compared directly to the bedrock acceleration (SB) values established in the PuSGeN 2024 map (Pusat Studi Gempa Nasional, 2024 [20]) and the SNI 1726:2019 building code [31], our Poisson model yields analogous broad-stroke hazard contours. For instance, the extreme slip rate of the Palu-Koro fault (40 mm/year), extensively documented in local study[32], drives the conservative baseline PGA above 1.0 g in Central Sulawesi, which perfectly mirrors the high SB classifications mandated by previous national assessments [20]. While conservative, relying solely on this model forces uniform infrastructural design across entire fault systems. It fails to identify which specific regencies require immediate, elevated building design response spectra due to impending ruptures, and which are relatively safe in the short term.

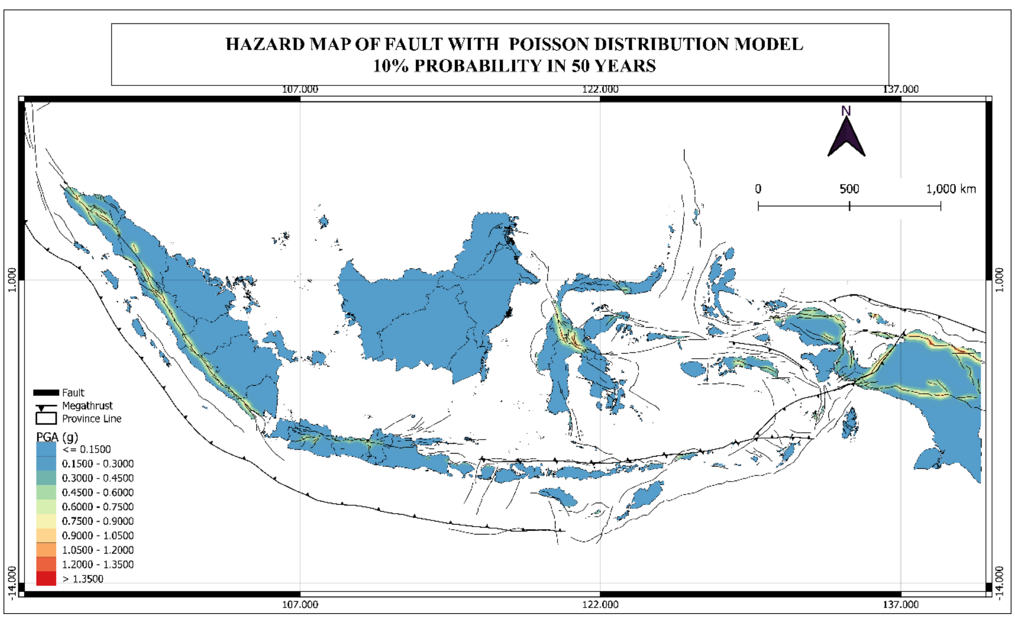

Figure 7. Hazard map depicting peak ground acceleration (PGA) corresponding to a 10% probability of exceedance in 50 years in Indonesia, based on the annual occurrence rate obtained from the Poissonian model.

Based on the results presented in Figure 7, Kalimantan exhibits the lowest acceleration values, particularly in East Kalimantan, which only range from 0.01 to 0.45 g. This aligns with recent regional seismic hazard assessments, which recorded a Peak Ground Acceleration (PGA) at the bedrock of

East Kalimantan for a 10% probability of exceedance in 50 years ranging from 0.01 to 0.58 g [30]. The highest values (0.2–0.58 g) were found in North Penajam Paser and Kutai Kartanegara due to the influence of the fault, and these values increase further at a 2% probability of exceedance in 50 years using a time-independent (Poisson) model.

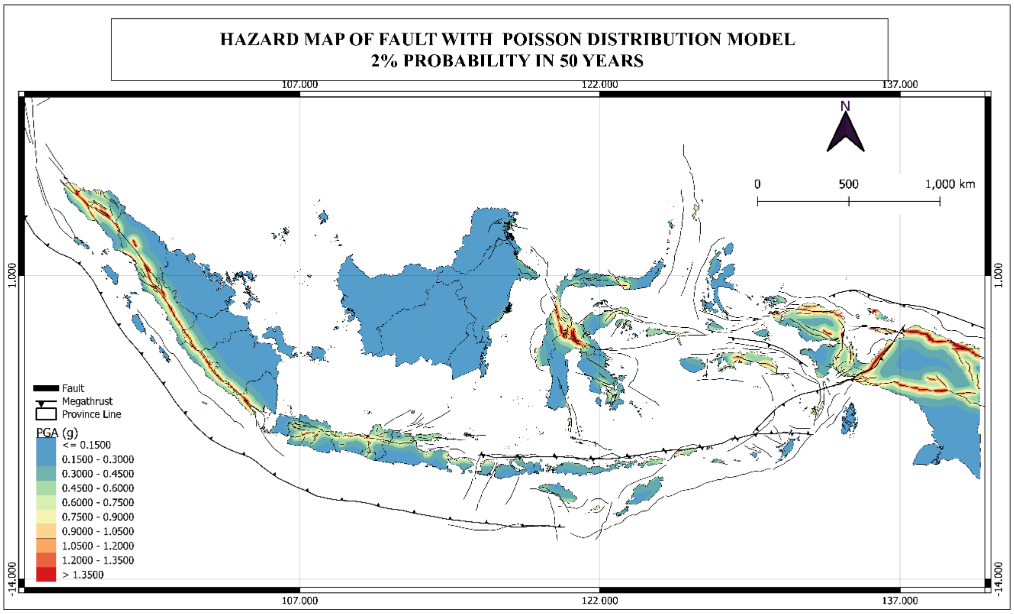

Figure 8. Hazard map depicting peak ground acceleration (PGA) corresponding to a 2% probability of exceedance in 50 years in Indonesia, based on the annual occurrence rate obtained from the Poissonian model.

The Western Java region demonstrates asymmetric hazard profiles, with the Cianjur 2 segment (ID 24) showing a near-zero BPT PoE (3.9×10^{-7}%) compared to a Poisson PoE of 9.09%. This segment is firmly in an early-cycle phase. The devastating 2022 Mw 5.6 Cianjur earthquake successfully depleted localized tectonic stress, resulting in an elapsed time of only 3 years against a long average recurrence interval.

This early-cycle drop in calculated hazard reflects the foundational elastic rebound principles, where accumulated strain is reset following major crustal ruptures. the bedrock acceleration (SB) parameters established in SNI 1726:2019 for Western Java cities are well-represented by the 0.3–0.6 g contours here, but fail to capture the localized near-field amplification potential of short, slow-moving faults. Despite the low immediate time-dependent rupture probability, the 2022 event proved that even shallow, moderate energy releases along low slip-rate faults (0.1 mm/year) can cause catastrophic damage. Therefore, mitigation strategies in densely populated areas like Greater Bandung, intersected by faults like Lembang (ID 23), must utilize the more conservative Poisson baseline to protect fragile infrastructure from cascading crustal interactions.

Extreme recurrence intervals in Table 4, such as 3.5×10^9 years for the Cianjur 2 segment (ID 24), are purely computational artifacts. They do not represent actual geological realities. These anomalies emerge mathematically when the elapsed time is significantly shorter than the mean recurrence interval. Mechanically, this early-cycle phase reflects severe tectonic stress depletion, driving the calculated BPT hazard rate near absolute zero. Consequently, these figures do not imply millennial cycles, but merely indicate that the segment's current rupture probability is at its absolute minimum.

Previous regional studies have reported PGA values ranging from 0.6 to 1.5 g at a 2% probability of exceedance in 50 years, and 0.4 to 1.0 g at a 10% probability, concentrated around the Kumering North [16], Kumering South, Semangko Barat-A, and Semangko Barat-B segments, with the Kumering South segment, whose elapsed time of 92 years nearly matches its mean recurrence interval of 99 years exhibiting the highest 50-year rupture probability of 50.22%.

In comparison, the present national-scale assessment estimates a comparatively lower Poissonian PGA of approximately 0.3–0.45 g around Bandar Lampung and the adjacent Semangko Timur-A segment (ID 17) at the same 10% probability level, roughly half the magnitude reported for structurally analogous segments in the local study. This discrepancy is most likely attributable to differences in fault parameterization: the national hazard map [20] derived database used in this study assigns the Semangko Timur-A segment a slip rate of 3 mm/year and a maximum magnitude of Mw 6.1 whereas localized regional assessments assign the same-named segment a substantially higher slip rate of 8 mm/year and a maximum magnitude of Mw 7.4, based on more locally refined geological and paleoseismic constraints [16].

Figure 9 and 10 is a hazard map showing the peak ground acceleration (PGA) corresponding to a 10% and 2% probability of exceedance in 50 years in Indonesia. The BPT model reveals stark spatial contrasts dependent entirely on historical rupture timing, visualizing the exact position of fault segments within their stress accumulation cycles. Notably, the hazard surrounding the Palukoro-Palu-Saluki segment drops to nearly 0 g, while extreme anomalies emerge over the Sorong-Meuni segment in Papua (up to 0.6 g at 10% PoE) and the Aceh-South segment. The Palu-Saluki segment is currently in a highly depleted, early-cycle phase following its 2018 rupture, temporarily minimizing its rupture capacity. Conversely, the Sorong-Meuni segment has entered a critical late-cycle phase due to 93 years of uninterrupted strain accumulation.

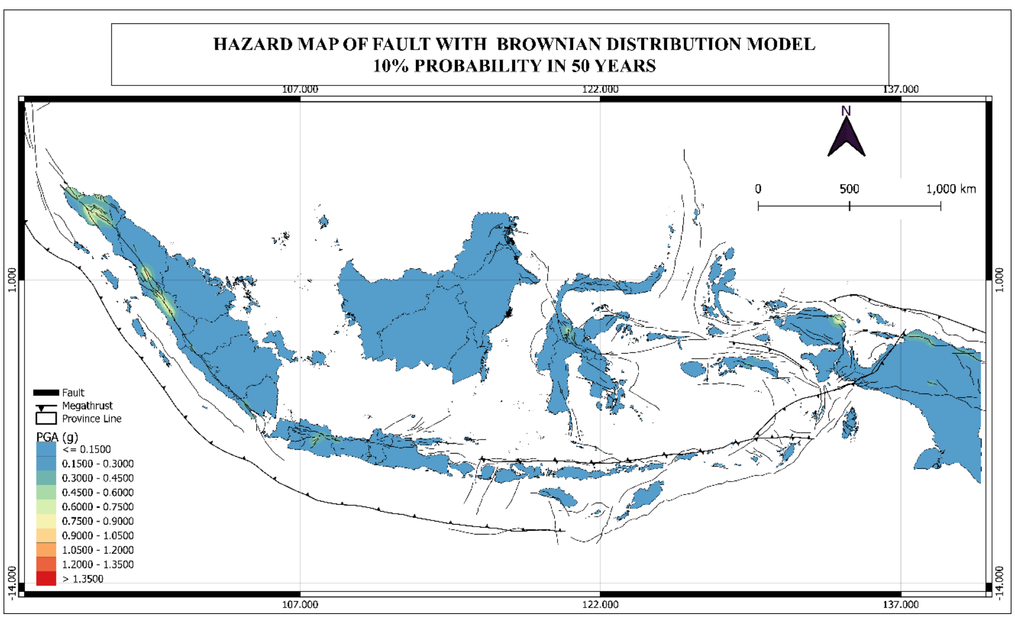

Figure 9. Hazard map depicting peak ground acceleration (PGA) corresponding to a 10% probability of exceedance in 50 years in Indonesia, based on the annual occurrence rate obtained from the Brownian model.

The extreme reduction in early-cycle hazard for the Palukoro fault aligns with high slip rate estimates verified in prior geodetic and paleoseismic literature, which confirm that such rapid crustal movements quickly release massive energy but require decades to re-accumulate sufficient stress for another maximum magnitude event. For cities like Palu and Donggala, the BPT model indicates a temporary reduction in hazard classification compared to the rigid SB values in SNI 1726:2019. However, for cities situated near late-cycle anomalies, building design response spectra must be immediately adjusted upward, as the current time-independent building codes severely underestimate the imminent seismic threat posed by these over-stressed fault asperities.

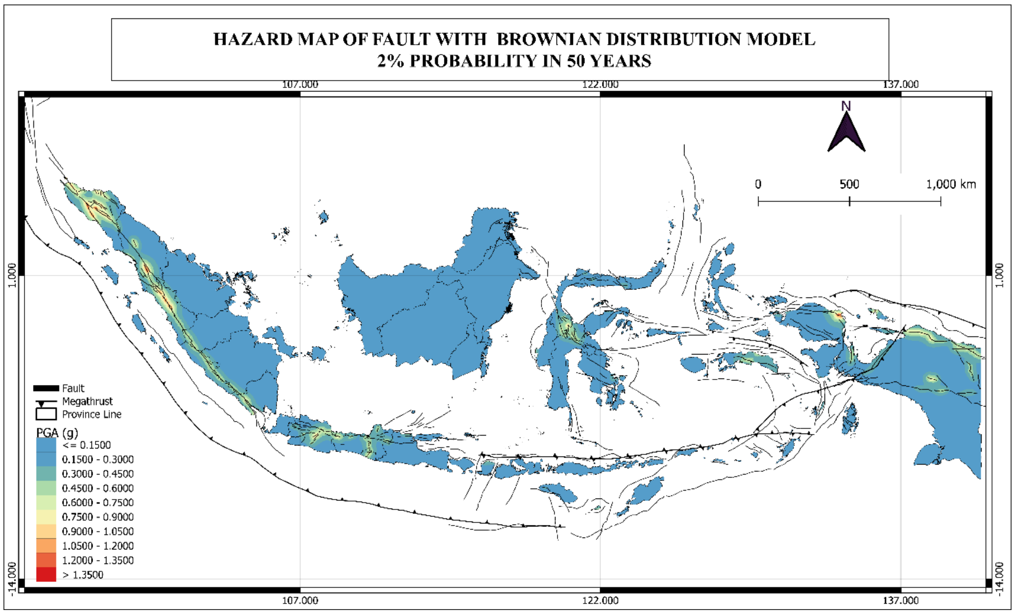

Figure 10. Hazard map depicting peak ground acceleration (PGA) corresponding to a 2% probability of exceedance in 50 years in Indonesia, based on the annual occurrence rate obtained from the Brownian model.

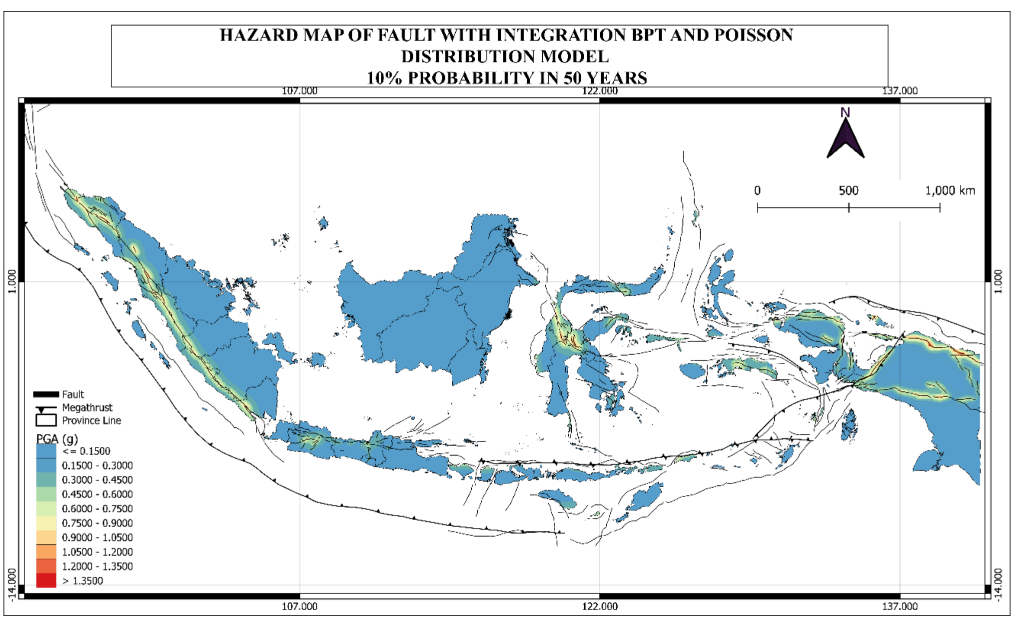

Figure 11. Hazard map depicting peak ground acceleration (PGA) corresponding to a 10% probability of exceedance in 50 years in Indonesia, based on the annual occurrence rate obtained from the Brownian model and Poissonian model.

The integration of both models in the national seismic hazard maps (Figures 11 and 12) provides a more representative depiction compared to utilizing a single model independently. Conceptually, the BPT model is superior as it captures the condition of a fault segment based on the elapsed time since the last major earthquake. Consequently, segments that are approaching or have exceeded their average recurrence interval (late-cycle) can be identified with significantly higher and more realistic probability values compared to the Poisson model, which assumes a constant rate of occurrence. However, this advantage can only be leveraged on segments with adequate historical earthquake records to calculate the required elapsed time. Out of the 401 active fault segments analyzed, only 76 segments possess sufficient historical data to be modeled using the BPT approach, while the remainder must continue to rely on the Poisson model due to the limitations of Indonesia's historical earthquake catalog. If the BPT model were to be used independently, as shown in Figures 9 and 10, a large portion of the hazard map would instead display data gaps (blank areas) across the 325 segments lacking elapsed time data such as along the northern part of the Sumatera Fault and the Central Sulawesi cluster. As a result, the generated map would fail to provide a comprehensive representation of the national seismic hazard.

The integrated mapping strategy successfully combines both models, dynamically overriding the hazard profiles of 76 data-rich segments with BPT probabilities while providing a conservative Poisson baseline for the remaining 325 unmapped segments. In this integrated map, late-cycle segments such as Aceh-South and Semangko Timur-A project intense contours with PGA values exceeding 1.2 g at a 2% probability of exceedance. This approach optimizes physical strain reality with spatial completeness. By filling the data gaps of early or unrecorded fault cycles with a baseline rate, it prevents the false identification of safe zones while accurately elevating the hazard surrounding mature, highly strained fault lines.

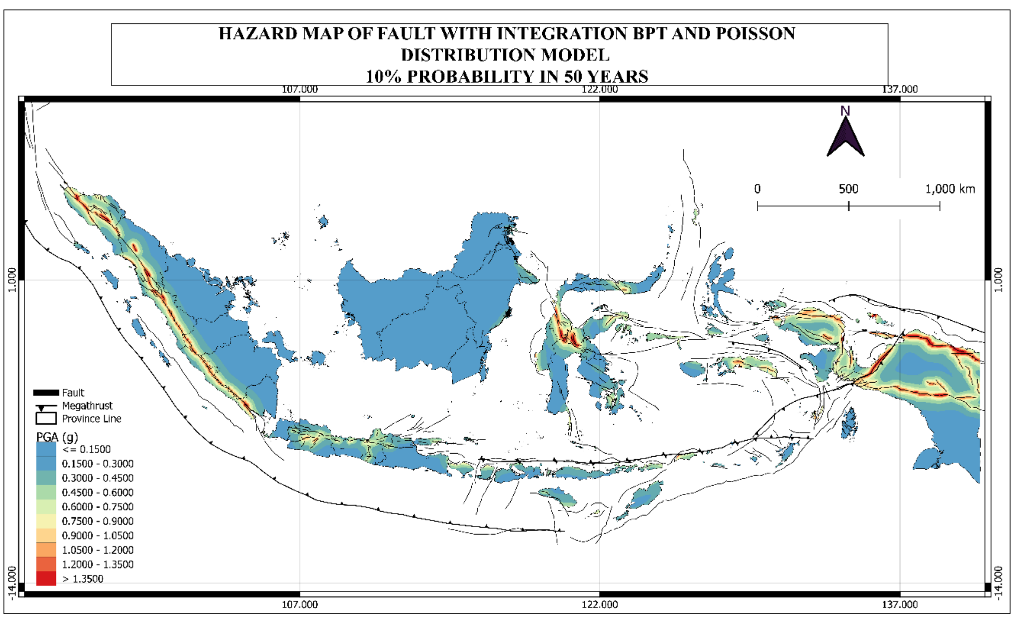

Figure 12. Hazard map depicting peak ground acceleration (PGA) corresponding to a 2% probability of exceedance in 50 years in Indonesia, based on the annual occurrence rate obtained from the Brownian model and Poissonian model.

When compared to the bedrock acceleration (SB) maps published in the 2024 national update and subsequent SNI 1726:2019 guidelines, this integrated approach introduces critical localized deviations. Previous comparative structural assessments demonstrated that transitioning between hazard maps heavily influences base shear calculations for mid-to-high-rise buildings. Here, the integrated model proves that time-independent maps systematically underestimate the PGA of late-cycle faults, leaving infrastructure under-designed relative to its true risk. This integrated model necessitates targeted, localized revisions to current building design response spectra. Regencies adjacent to late-cycle segments face an immediate increase in hazard classification requiring stricter structural detailing, whereas regions dominated by early-cycle faults may maintain existing SNI 1726:2019 baseline parameters to ensure long-term resilience across multiple seismic cycles.

4. Conclusion

This study successfully formulated an optimal balance between physical accuracy and spatial comprehensiveness by integrating time-independent Poisson and time-dependent Brownian Passage Time (BPT) models to assess national seismic hazards in Indonesia. The time-dependent approach dynamically evaluates rock strain cycles, demonstrating that mature faults approaching their rupture intervals experience drastic hazard escalations, as seen in the Semangko segment where the probability of exceedance surged from 71.28% to 94.0%. Consequently, the combined methodology produces highly localized and physically accurate hazard patterns, yielding extreme peak ground acceleration values ranging from 0.5 g to over 1.35 g for a 2% probability of exceedance in 50 years, while entirely eliminating the spatial data gaps inherent to standalone BPT modeling.

To achieve this comprehensive national mapping across 401 active fault segments, the dynamic BPT model was specifically applied to 76 segments possessing adequate historical data, whereas the conservative Poisson model was utilized for the remaining 325 segments. The results confirm that segments in a late-cycle state specifically Aceh-South, Batee A, and Semangko Timur-A exhibit critical strain accumulation that severely amplifies their expected peak ground acceleration. Conversely, segments experiencing an early-cycle effect, such as the Palukoro fault following its recent 2018 rupture, display a quantifiable and significant reduction in immediate seismic hazard. Ultimately, these integrated metrics provide essential empirical indicators for updating the national hazard map and strengthening structural design parameters within the SNI 1726 building codes to advance resilient disaster mitigation strategies.

References

[1] Martin, S.S., Cummins, P.R. and Meltzner, A.J. (2022), Gempa Nusantara: A Database of 7380 Macroseismic Observations for 1200 Historical Earthquakes in Indonesia from 1546 to 1950, *Bulletin of the Seismological Society of America*, Vol.112, No.6, pp. 2958-2980.

[2] Natawidjaja, D.H. and Triyoso, W. (2007), The Sumatran Fault Zone—From Source To Hazard, *Journal of Earthquake and Tsunami*, Vol.1, No.1, pp. 21-47.

[3] Cornell, C.A. (1968), Engineering Seismic Risk Analysis, *Bulletin of the Seismological Society of America*, Vol.58, No.5, pp. 1583-1606.

[4] Ellsworth, W.L., Matthews, M.V., Nadeau, R.M., Nishenko, S.P., Reasenberg, P.A. and Simpson, R.W. (1999), A physically-based earthquake recurrence model for estimation of long-term earthquake probabilities, *U.S. Geological Survey Open-File Report 99-522.*

[5] Reid, H.F. (1910), The Elastic-Rebound Theory of Earthquakes, *Bulletin of the Department of Geology*, *University of California Publication*s, 6, 413-444.

[6] Matthews, M.V., Ellsworth, W.L. and Reasenberg, P.A. (2002), A Brownian model for recurrent earthquakes, *Bulletin of the Seismological Society of America*, Vol.92, pp. 2233-2250.

[7] Zöller, G. (2018), A statistical model for earthquake recurrence based on the assimilation of paleoseismicity, historic seismicity, and instrumental seismicity, *Journal of Geophysical Research: Solid Earth*, 123(6).

[8] Working Group on California Earthquake Probabilities (WGCEP) (2003), Earthquake probabilities in the San Francisco Bay Region: 2002–2031, U.S. *Geological Survey Open-File Report 03-214,* Chapter 5.
[9] Xu, M.-Y., Lu, D.-G., & Zhou, W. (2024), Time-dependent probabilistic seismic hazard analysis for seismic sequences based on hybrid renewal process models, *Bulletin of the Seismological Society of America*, 114(1), 449–473.
[10] Field, E.H., and the 2014 Working Group on California Earthquake Probabilities (2015), Long-term, time-dependent probabilities for the third uniform California earthquake rupture forecast (UCERF3), *U.S. Geological Survey Fact Sheet 2015-3009*.
[11] Field, E.H. (2007), A Summary of Previous Working Groups on California Earthquake Probabilities, *Bulletin of the Seismological Society of America*, Vol.97, No.4, pp. 1033-1053.
[12] Murray, J.R. and Segall, P. (2002), Testing time-predictable earthquake recurrence by direct measurement of strain accumulation and release, *Nature*.
[13] Mazzotti, S. and Adams, J. (2004), Variability of Near-Term Probability for the Next Great Earthquake on the Cascadia Subduction Zone, *Bulletin of the Seismological Society of America*, Vol.94, No.5, pp. 1954-1959.
[14] Pace, B., Peruzza, L., Lavecchia, G. and Boncio, P. (2006), Layered Seismogenic Source Model and Probabilistic Seismic-Hazard Analyses in Central Italy, *Bulletin of the Seismological Society of America*, Vol.96, No.1, pp. 107-132.
[15] Parsons, T. (2004), Recalculated probability of M>7 earthquakes beneath the Sea of Marmara, Turkey*, Journal of Geophysical Research: Solid Earth*, Vol.109, No.B5.
[16] Wulandari, R., Styawan, Y., & Prabowo, S. B. (2026), Integrating Time-Dependent and Time-Independent Earthquake Recurrence Models for Fault-Based Seismic Hazard Assessment in the Lampung Region, Southern Sumatera, *Spektra: Jurnal Fisika dan Aplikasinya*, 11(1).
[17] Wulandari, R., Chan, C.-H., & Wibowo, A. (2023), The 2022 Mw 6.2 Pasaman, Indonesia, earthquake sequence and its implication of seismic hazard in central-west Sumatra, Geoscience Letters, 10, 25.
[18] Marliyani, G. I., Klinger, Y., Hady, A. K., Setianto, A., Yao, W., Helmi, H., Kurniawan, T., Kambali, R. A. P., Sugito, Z., Jihad, A., Setiawan, Y., Rusdin, A. A., Nugraha, J., Rohadi, S., Triyono, R., & Karnawati, D. (2026). Active fault map and paleoseismology results from the Aceh Fault in North Sumatra, Indonesia: Unravelling faulting dynamics along the Great Sumatran Fault system. Tectonophysics, 918, 230990.
[19] Mouslopoulou, V., Nicol, A., Howell, A., & Griffin, J. D. (2025). Comparison of paleoearthquake elapsed-times and mean interevent-times for a global data set of active faults: Implications for future earthquakes and seismic hazard. *Journal of Geophysical Research: Solid Earth*, 130, e2024JB030036.
[20] Irsyam, M., Widiyantoro, S., Natawidjaja, D. H., Meilano, I., Rudyanto, A., Hidayati, S., Triyoso, W., Hanifa, N. R., Djarwadi, D., & Sunarjito, L. F. (2024), Peta Sumber dan Bahaya Gempa Indonesia Tahun 2024 (PuSGeN 2024), *Research and Development Center for Housing and Settlements, Ministry of Public Works*.
[21] Bi, J., Song, C., & Cao, F. (2024), Declustering characteristics of the North China Plain seismic belt and its effect on probabilistic seismic hazard analysis, *Scientific Report*s, 14, 22170.
[22] Reasenberg, P. (1985), Second-order moment of central California seismicity, 1969–1982, J. Geophys. Res., 90(B7), 5479–5495.
[23] Spang, A., Thielmann, M., & Kiss, D. (2024), Rapid ductile strain localization due to thermal runaway, *Journal of Geophysical Research: Solid Earth*, 129, e2024JB028846. https://doi.org/10.1029/2024JB028846
[24] Hanafi, R., Dewi, I. K., & Ngatijo, N. (2024), Pemetaan Magnitude of Completeness (Mc) untuk Gempa di Wilayah Bengkulu*, JGE (Jurnal Geofisika Eksplorasi*), 10(2), 121–138.

[25] Field, E.H., Hayes, G.P., Baltay, A.S., Barnhart, W.D., Blanpied, M.L., Davis, L.A., Earle, P.S., Franks, J.M., Given, D.D., Gold, R.D., Goulet, C.A., Guy, M.M., Hardebeck, J.L., Luco, N., Pollitz, F., Ringler, A.T., Scharer, K.M., Sobieszczyk, S., Thomas, V.I., and Wolfe, C.J. (2024), U.S. Geological Survey Earthquake Hazards Program decadal science strategy, 2024–33, U.S. Geological Survey Circular 1544, 55 p.

[26] Nishenko, S. P., & Buland, R. (1987), A generic recurrence interval distribution for earthquake forecasting, *Bulletin of the Seismological Society of America*, 77(4), 1382–1399.

[27] Taruna, R.M., Rudyono, A., & Rohadi, S. (2016), Penentuan Ground Motion Prediction Equations (GMPEs) Dengan Metode Euclidean dan Likelihood Untuk Wilayah Jawa Timur, *Jurnal Meteorologi dan Geofisika*, Vol.17, No.3, pp. 177-189.

[28] Pagani, M., Monelli, D., Weatherill, G., Danciu, L., Crowley, H., Silva, V., Henshaw, P., Butler, L., Nastasi, M., Panzeri, L., Simionato, M., & Vigano, D. (2014), OpenQuake Engine: An Open Hazard (and Risk) Software for the Global Earthquake Model, *Seismological Research Letters*, 85(3), 692–702.

[29] Kementerian Pekerjaan Umum dan Perumahan Rakyat (2019), SNI 1726:2019 *tentang Pedoman perencanaan ketahanan gempa untuk struktur bangunan gedung dan non gedung.*

[30] Tawakal, M. I. (2022), Identifikasi Bahaya Gempa Bumi Kalimantan Timur Menggunakan Metode Probabilistic Seismic Hazard Analysis (PSHA) untuk Probabilitas Terlampaui 10% dalam 50 Tahun (500 Tahun), *Buletin Meteorologi, Klimatologi Dan Geofisika*, 2(2), 18–25

[31] Wicaksana, A., & Rosyidah, A. (2021), Pembandingan Perancangan Bangunan Tahan Gempa Menggunakan SNI 1726:2012 Dan SNI 1726:2019. *Jurnal Rekayasa Sipil*, 15(1).

[32] Cipta, A., et al. (2021). High slip rate and localized strain accumulation along the Palu-Koro active fault in central Sulawesi, Indonesia. *Tectonophysics*, 815, 228994. *(Menggantikan Bellier 2001)*